International Journal of Engineering Research and Technology. ISSN 0974-3154 Volume 10, Number 1 (2017)

Mathematical Modelling of Fluidized Bed Drying

Prof. D.N.Deomore[1]
[1]*Assosciate Professor, Dept. of Mechanical Engg.,*
D.Y.Patil College of Engineering& Technology, Kolhapur,
Maharashtra, India

Prof. (Dr.) R.B.Yarasu[2]
[2]*Professor, Government College of Engineering, Nagpur,*
Maharashtra, India

Abstract
Of all the unit operations used by the process industries, drying is probably the oldest and the most common one found in diverse fields such as agricultural, chemical, food, pharmaceutical, pulp and paper, mineral, polymer, ceramic, and textile industries. An attempt is made in the present paper to provide mathematical modelling of Fluidized Bed Drying. Before performing drying calculation on wheat certain assumptions were made and drying condition were determined. The wheat was assumed to be spherical of 3.66mm diameter, particle density of 1215 kg/m3 and a total weight to be dried was 50gm.moisture content of the wheat is initially set to replicate freshly harvested condition i.e. 0.25 kg moisture/kg dry basis. Before starting the drying procedure the temperature of wheat and ambient air is presumably equalized and moisture diffusion to the surface of wheat is assumed to be uniform..

Keywords: Fluidized bed.

1. Introduction

Fluidization is a process where a bed of loosely packed solid particles takes on some of the properties of a fluid when a gas is blown vertically upwards through it. Introducing a gas (gas-solid systems) from the bottom of a column containing solid particles via a gas distributor can cause the particles vibration and expansion in order to compensate the drag force exerted on them by the gas stream. Upon increasing the gas velocity, a point is reached at which the drag force equals the weight of the particles and the bed is said to be fluidized.

Fluidized beds are used as a technical process which has the ability to enhance high level of gases and solids contact. In a fluidized bed a particular set of basic properties can be used, indispensable to modern process and chemical engineering.

According to the ASAE S448 DEC98 standard the particles layer on the bed shall not be more than 3 with least 0.31 meters per second of airflow rate. The drying area was set to be 0.096 square meters. The dryer wall will be adiabatic with no conduction or radiation to the material. The temperature range of the dryer may vary from 290 Kelvin to 360 Kelvin. Temperatures above 360 Kelvin are not explored due to possible damage to the wheat grain. The ambient air temperature shall be constant and equal to 290K. Although the transition phase between the constant rate and falling rate periods is far more complex than shown in the calculations a stepwise transition phase is assumed instead of a continuous transition. The mathematical model will not take into account the kinetic or potential energy of the wheat or drying air at any given time.

2. Literature Review

R. Sivakumar, R. Saravanan, A. ElayaPerumal, S. Iniyan (2016)summarized the importance of FBD drying in combination with hybrid FBD drying techniques in moisture reduction of various agricultural products. The impact of various operating parameters on the product quality, color, texture and resultant nutritional value is discussed, with possible adaption of multi-effect systems.

S. Syahrul, I. Dincer b, F. Hamdullahpur (2002)observed that the thermodynamic efficiency of the fluidized bed dryer was the lowest at the end of the drying process in conjunction with the moisture removal rate. The inlet air temperature has a strong effect on thermodynamic efficiency for wheat, but for corn, where the diffusion coefficient depends on the temperature and the moisture content of particles, an increase in the drying air temperature did not result in an increase of the efficiency. Furthermore, the energy and exergy efficiencies showed higher values for particles with high initial moisture content while the effect of gas velocity varied depending on the particles. A good agreement was achieved between the model predictions and the available experimental results.

WijithaSenadeera, Bhesh R. Bhandari, Gordon Young , BanduWijesinghe(2002) Three different particular geometrical shapes of parallelepiped, cylinder and sphere were taken from cut green beans (length: diameter ¼ 1:1, 2:1 and 3:1) and potatoes (aspect ratio ¼ 1:1, 2:1 and 3:1) and peas, respectively. Their drying behavior in a fluidized bed was studied at three different drying temperatures of 30, 40 and 50 ^{0}C (RH ¼ 15%). Drying curves were constructed using non-dimensional moisture ratio (MR) and time and their behavior was modeled using exponential (MR = exp(kt)) and Page (MR = exp(-kt^{n})) models. The effective diffusion coefficient of moisture transfer was determined by Fickian method using uni and three-dimensional moisture movements. The diffusion coefficient was least affected by the size when the moisture movement was considered three dimensional, whereas the drying temperature had a significative effect on diffusivity as expected. The drying constant and diffusivity coefficients were on the descending order for potato, beans and peas. The Arrhenius activation energy for the peas was also highest, indicating a strong barrier to moisture movement in peas as compared to beans and skinless cut potato pieces.

3. Drying of Single Large Particles

In this section the drying process of wheat particles having moisture contents more than 30% is dealt. For this liquid and bound water are required to be distinguished because they migrate through the particle differently.

3.1 Theory and Model Description

In this section drying is considered as a process where the source term is based on the vapor concentration at the particle surface and local gas environment. In this study wheat beans with moisture content below 10% is taken thus water is assumed to be bound water only. Conduction is assumed to be only energy transport mechanism inside a spherical particle while neglecting reaction enthalpy, heat transport by water diffusion and condensation. In that case the energy transport equation is solved inside each particle as given in eq. (30), although different boundary conditions at the particle surface apply due to the different drying approach used.

$$\frac{(\partial(\rho cT)}{\partial t} = \rho c \frac{\partial T}{\partial t} = \frac{1}{r^2}\frac{\partial}{\partial r}\left(\lambda r^2 \frac{\partial T}{\partial r}\right) + \dot{\omega} \quad \text{..... (30)}$$

$$\frac{\partial T_p}{\partial r}\Big| = 0 \qquad -\lambda_p \frac{\partial T_p}{\partial r}\Big| r = 1 = h(T_p - T_f) + K(C_S - C_f)\Delta H_{evap} \quad \text{..... (31)}$$

h= convective heat transfer
k= mass transfer coefficient

Both heat and mass transfer coefficient are derived from the Colburn (or Colburn-Chilton) analogy, where the Colburn j-factor" has been obtained from the Gupta and Thodo's correlation [156] for fixed and fluidized beds. The convective heat and mass transfer coefficients are then expressed as:

$$h = 2.06Re^{-0.575}\left|\frac{u_f - u_p}{\epsilon}\right| C_P f_\rho P \left(\frac{\lambda_f}{C_P, f u_f}\right)^{2/3} \quad \text{..... (32)}$$

Rep = the particle Reynolds number.

Evaporation takes place only at the surface of the particle and the source term $\dot{\omega}$ in eq. (30) is zero. Liquid water transport within the wheat is modeled via diffusion and the conservation equation for water without considering water generation due to condensation is given by

$$\frac{\partial Y_{water}\ (r,t)}{\partial t} = D\left[\frac{\partial^2 water}{\partial r^2} + \frac{2}{r}\frac{\partial Y_{water}}{\partial r}\right] \quad \text{..... (33)}$$

The effective diffusion coefficient *D* is set to a constant value and has not been modified for all simulations. The boundary conditions at the particle centre (r = 0) and at the particle surface (r = R) are given as:

$$\frac{\partial Y_{water}}{\partial r}\Big| = 0 \ - D_\rho P \frac{\partial Y_{water}}{\partial r}\Big| r = R \quad = K(C_s - C_f) \quad \text{..... (34)}$$

C_f= the vapor concentration in the fluid phase
C_s = the vapor concentration at the wheat surface.

The vapor concentration at the surface can be described as a function of material, temperature and water concentration according to:

$$c_s = a_w(Y_{water}, S, TP_s)C_{sat}, S \quad \text{..... (35)}$$

C_{sat}; S = vapor saturation concentration at the particle surface
a_w = the water activity obtained from Iglesias and Chirife [157].

4. Discretization of Differential Equations

After derivation of fundamental differential equation next step was the discretization of these equations using a proper method. The derivation of discretization can be done in many ways thus based on the nature of the problem a suitable method must be chosen. Some of these are mentioned below:

1. Taylor series expansion
2. Polynomial fitting
3. Integral method
4. Control volume approach

Taylor series expansion and control volume approaches are most commonly used methods for various types of differential equation. For discretization of equation and application in numerical problem both methods were considered. Control volume approach was found to have better convergence and stability than Taylor series expansion especially in high temperature where there is a rise in nonlinearity of process. Thus for numericalimplementation of partial differential equation control volume formulation was chosen. The calculation domain was divided in to several non-overlapping control volumes such that each grid point was surrounded by a control volume. In order to evaluate the required integrals piecewise profiles expressing the variation of dependent variable between grid points were used.

4.1 Interstitial Gas Phase

First of all the mass transfer equation for interstitial gas phase is considered. As mentioned before the derived equation for mass and energy for the interstitial gas belongs to the hyperbolic type of partial differential equation like upwind method, Lax-Wendroff method, MacCornack method and so forth. The variation in the solution's quality by using various schemes is negligible except for some exceptions. Stability criteria are the most important characteristics of any scheme. The solution provided by implicit approach has higher stability than those of explicit approach thus this approach was used for the differential equation discretization under an appropriate scheme
Unsteady, convection and sources included in the interstitial gas equation are termed as

$$\frac{\partial}{\partial t}(\rho_a X_i \varepsilon_i) + \frac{\partial}{\partial y}(\rho_a X_i \varepsilon_i u_i) = \frac{\rho_a k_p (X_p - X_i) 6\varepsilon_p}{d_p} + \rho_a K_{ib} \varepsilon_b (X_b - X_i) \ldots\ldots\ldots\ldots\ldots \quad (54)$$

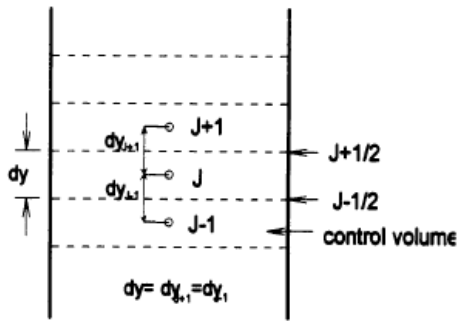

Figure 4.2 Control Volumes and Grid Point Cluster inside the Bed

Grid point cluster for the derivation of the discretization equation as shown in fig 7.1 was used. The focus of attention was grid point j having grid point j+1 and j-1 as its neighbor. Faces of the control volumes were denoted by j+1/2 and j-1/2 and are shown by the dashed lines. Integrating eq. (54) over the control volume gave:

$$\int_{j-\frac{1}{2}}^{j+\frac{1}{2}} \int_t^{t+\Delta t} \frac{\partial}{\partial t}(\rho_a X_i \varepsilon_i)\, dt dy + \int_t^{t+\Delta t} \int_{j-\frac{1}{2}}^{j+\frac{1}{2}} \frac{\partial}{\partial y}(\rho_a X_i \varepsilon_i u_i)\, dy dt = \int_{j-1/2}^{j+1/2} \int_t^{t+\Delta t} \frac{\rho_a k_p (X_p - X_i) 6\varepsilon_p}{d_p} dt dy + \int_{j-1/2}^{j+1/2} \int_t^{t+\Delta t} \rho_a K_{ib} \varepsilon_b (X_b - X_i)\, dt dy \ldots\ldots\ldots\ldots \quad (55)$$

When the nature of term is considered base for integration order selection. For the unsteady term, the first term on the left side of eq (54), we shall assume that the grid point value of variables prevails throughout the control volume then,

$$\int_{j-\frac{1}{2}}^{j+\frac{1}{2}} \int_t^{t+\Delta t} \frac{\partial}{\partial t}(\rho_a X_i \varepsilon_i)\, dt dy = [(\rho_a X_i \varepsilon_i)^{n+1,j} - (\rho_a X_i \varepsilon_i)^{n,j}]\Delta y \ldots\ldots\ldots\ldots\ldots\ldots \quad (56)$$

Integration for the convection yields:

$$\int_t^{t+\Delta t} \int_{j-\frac{1}{2}}^{j+\frac{1}{2}} \frac{\partial}{\partial y}(\rho_a X_i \varepsilon_i u_i)\, dy dt = \int_t^{t+\Delta t} [(\rho_a X_i \varepsilon_i u_i)^{j+\frac{1}{2}} - (\rho_a X_i \varepsilon_i u_i)^{j-\frac{1}{2}}] dt \ldots\ldots\ldots \quad (57)$$

Selection of a value for variables at j+1/2 and j-1/2 should be done. In this work we have used upwind approach for the convection term discretization. Since it was assumed that the interstitial gas in the plug flow, the gas velocity is always upwards. So j+1/2 was replaced with j and j-1/2 with j-1

As variables proved to be varying with time from t to t+Δt an assumption was made by selecting an implicit approach for stability preservation. The result thus found were

$$\int_t^{t+\Delta t} [(\rho_a X_i \varepsilon_i u_i)^{j+\frac{1}{2}} - (\rho_a X_i \varepsilon_i u_i)^{j-\frac{1}{2}}] dt = [(\rho_a X_i \varepsilon_i)^{n+1,j} - (\rho_a X_i \varepsilon_i u_i)^{n+1,j-1}]\Delta t \ldots. \quad (58)$$

For the right side terms of eq (54) grid point values of variables were assumed to prevail throughout the control volume and implicit approach can be used for the variation with time. The final discretization form of the mass balance equation for the interstitial gas is:

$$[(\rho_a X_i \varepsilon_i)^{n+1,j} - (\rho_a X_i \varepsilon_i)^{n,j}]\Delta y + [(\rho_a X_i \varepsilon_i)^{n+1,j} - (\rho_a X_i \varepsilon_i u_i)^{n+1,j-1}]\Delta t = [\frac{\rho_a k_p (X_p - X_i) 6\varepsilon_p}{d_p} + \rho_a K_{ib} \varepsilon_b (X_b - X_i)]\Delta y \Delta t \ldots\ldots\ldots\ldots\ldots\ldots \quad (59)$$

Since energy equation in the interstitial gas is same thus a similar approach can be applied. The discretized form of the energy equation is

$$[(\rho_a C_i \varepsilon_i T_i)^{n+1,j} - (\rho_a C_i \varepsilon_i T_i)^{n,j}]\Delta y + [(\rho_a C_i \varepsilon_i T_i)^{n+1,j} - (\rho_a C_i \varepsilon_i u_i T_i)^{n+1,j-1}] = [h_p (T_i - T_i) \frac{6\varepsilon_p}{d_p} + \rho_a k_p (X_p - X_i) \frac{6\varepsilon_p}{d_p} C_v (T_p - T_i) + H_{ib} \varepsilon_b (T_b - T_i) + \rho_a K_{ib} \varepsilon_b (X_b - X_i) C_v (T_b - T_i) + h_s (T_s - T_i) \frac{(1-\varepsilon_p}{d_{tan\ K}}]^{n+1,j} \Delta y \Delta t \ldots\ldots\ldots\ldots\ldots\ldots\ldots \quad (60)$$

4.2 The Bubble Phase

Just like interstitial gas phase the mass and energy equation for the bubble phase also belongs to the hyperbolic type of partial differential equation. A similar process was used to discretize the mass and energy equation for this phase:

$$[(\rho_a X_b \varepsilon_b)^{n+1,j} - (\rho_a X_b \varepsilon_b)^{n,j}]\Delta y + [(\rho_a X_b \varepsilon_b u_b)^{n+1,j} - (\rho_a X_b \varepsilon_b u_b)^{n,j}]\Delta t = [\rho_a K_{ib} \varepsilon_b (X_i - X_b)]^{n+1,j} \Delta y \Delta t \ldots\ldots\ldots\ldots\ldots\ldots\ldots\ldots \quad (61)$$

And for the energy balance it is:

$$[(\rho_a C_i \varepsilon_b T_b)^{n+1,j} - (\rho_a C_i \varepsilon_b T_b)^{n,j}]\Delta y + [(\rho_a u_b \varepsilon_b T_b)^{n+1,j} - (\rho_a \varepsilon_b u_b T_b)^{n,j}]\Delta t = [H_{ib} \varepsilon_b (T_i - T_b) + \rho_a K_{ib} \varepsilon_b (X_i - X_b) C_v (T_i - T_b)]^{n+1,j} \Delta y \Delta t \ldots\ldots \quad (62)$$

4.3 The Solid Phase

The mass and energy equation for the solid phase belong to the parabolic type of partial differential equation. Like the approach for the hyperbolic system of equation an implicit approach is used in the discretization of the solid phase equation

Another difference between the characteristics of solid phase and gas phase equation is the type of coordinate used in any case. For discretization of the solid phase equations spherical coordinates are used since particles are spherical in shape unlike gas phase discretization in which Cartesian coordinates were used. One dimensional mass diffusion equation considered for discretization formula development in spherical coordinates is shown below

$$\frac{\partial M_p}{\partial t} = \frac{1}{r^2}\frac{\partial}{\partial r}\left(r^2 D \frac{\partial M_p}{\partial r}\right) \ldots\ldots\ldots\ldots\ldots\ldots\ldots\ldots\ldots\ldots\ldots \quad (63)$$

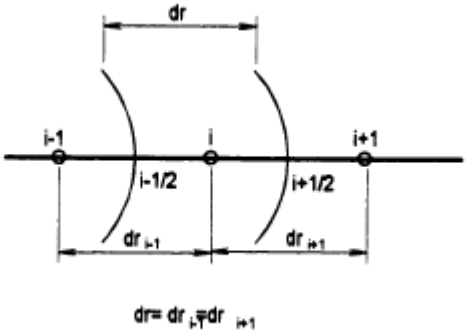

Figure 4.3 Control volume and grids in spherical coordinates

Multiply $4\pi r^2$ in equation 63 in order to obtain discretization equation after that integrate it over the control volume and time interval from t-t+Δt

$$\int_{i-1/2}^{i+1/2}\int_{t}^{t+\Delta t} 4\pi r^2 \frac{\partial M_p}{\partial t} dt dr = \int_{t}^{t+\Delta t}\int_{i-1/2}^{i+1/2} 4\pi \frac{\partial}{\partial r}\left(r^2 D \frac{\partial M_p}{\partial r}\right) dr dt \ldots\ldots\ldots\ldots\ldots\ldots \quad (64)$$

Grid-point value of M_p is assumed to prevail throughout the control volume, then

$$\int_{i-1/2}^{i+1/2}\int_{t}^{t+\Delta t} 4\pi r^2 \frac{\partial M_p}{\partial t} dt dr = \left(M_{P_i}^{n+1} - M_{P_i}^{n}\right)\Delta V \ldots\ldots\ldots\ldots\ldots\ldots\ldots\ldots \quad (65)$$

Now integrating the equation over control volume yielding

$$\int_{t}^{t+\Delta t}\int_{i-1/2}^{i+1/2} \frac{\partial}{\partial r}\left(r^2 D \frac{\partial M_p}{\partial r}\right) dr dt = \int_{t}^{t+\Delta t}\left[\frac{r_{i+1/2}^2 D_{i+1/2}\left(M_{P_i+1} - M_{P_i}\right)}{\delta r_{i+1}} - \frac{r_{i-1/2}^2 D_{i-1/2}\left(M_{P_i} - M_{P_{i-1}}\right)}{\delta r_{i-1}}\right] 4\pi dt \ldots\ldots\ldots\ldots \quad (66)$$

Variation of M_p from time t to t+Δt is assumed.

$$\int_{t}^{t+\Delta t}\int_{i-\frac{1}{2}}^{i+\frac{1}{2}} \frac{\partial}{\partial r}\left(r^2 D \frac{\partial M_p}{\partial r}\right) dr dt = f\left[\frac{r_{i+\frac{1}{2}}^2 D_{i+\frac{1}{2}}\left(M_{P_i+1}^{n+1} - M_{P_i}^{n+1}\right)}{\delta r_{i+1}} - \frac{r_{i-\frac{1}{2}}^2 D_{i-\frac{1}{2}}\left(M_{P_i}^{n+1} - M_{P_{i-1}}^{n+1}\right)}{\delta r_{i-1}}\right]\Delta t + (1-f)\left[\frac{r_{i+\frac{1}{2}}^2 D_{i+\frac{1}{2}}\left(M_{P_i+1}^{n} - M_{P_i}^{n}\right)}{\delta r_{i+1}} - \frac{r_{i-\frac{1}{2}}^2 D_{i-\frac{1}{2}}\left(M_{P_i}^{n} - M_{P_{i-1}}^{n}\right)}{\delta r_{i-1}}\right]\Delta t \ldots \quad (67)$$

Solving the equation produces

$$\frac{\left(M_{P_i}^{n+1} - M_{P_i}^{n}\right)\Delta V}{4\pi\Delta t} = f\left[\frac{r_{i+\frac{1}{2}}^2 D_{i+\frac{1}{2}}\left(M_{P_i+1}^{n+1} - M_{P_i}^{n+1}\right)}{\delta r_{i+1}} - \frac{r_{i-\frac{1}{2}}^2 D_{i-\frac{1}{2}}\left(M_{P_i}^{n+1} - M_{P_{i-1}}^{n+1}\right)}{\delta r_{i-1}}\right]\Delta t +$$

$$(1-f)\left[\frac{r_{i+\frac{1}{2}}^2 D_{i+\frac{1}{2}}\left(M_{P_i+1}^{n} - M_{P_i}^{n}\right)}{\delta r_{i+1}} - \frac{r_{i-\frac{1}{2}}^2 D_{i-\frac{1}{2}}\left(M_{P_i}^{n} - M_{P_{i-1}}^{n}\right)}{\delta r_{i-1}}\right]\Delta t \ldots\ldots\ldots\ldots\ldots\ldots\ldots\ldots \quad (68)$$

To obtain the boundary condition integrates eq10 over the surface grid considering the effect of surface mass transfer with the interstitial gas.

$$\int_{i-1/2}^{i}\int_{t}^{t+\Delta t} 4\pi r^2 \frac{\partial M_p}{\partial t} dt dr = \int_{t}^{t+\Delta t}\int_{i-1/2}^{i} 4\pi \frac{\partial}{\partial r}\left(r^2 D \frac{\partial M_p}{\partial r}\right) dr dt \ldots\ldots\ldots\ldots \quad (69)$$

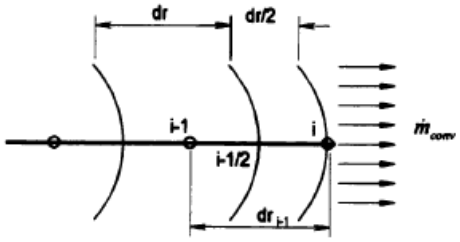

Figure 4.4 Half control volume at boundary condition
The integration results are as follows

$$\left(M_{P_i}^{n+1} - M_{P_i}^{n}\right)\rho_p \Delta V_i = \int_{t}^{t+\Delta t}\left(\dot{m}_{conv} - \left(\rho_p A_{i-1/2} D_{i-1/2}\left(\frac{\partial M_p}{\partial r}\right)_{i-1/2}\right)\right) dt \ldots\ldots\ldots\ldots \quad (70)$$

The final form of discretization of boundary layer is

$$\left(M_{P_i}^{n+1} - M_{P_i}^{n}\right)\frac{\Delta V}{4\pi\Delta t} = -f\left[\frac{A_{i-\frac{1}{2}} D_{i-\frac{1}{2}}\left(M_{P_i}^{n+1} - M_{P_{i-1}}^{n+1}\right)}{\delta r_{i-1}}\right] - (1-f)\left[\frac{A_{i-\frac{1}{2}} D_{i-\frac{1}{2}}\left(M_{P_i}^{n+1} - M_{P_{i-1}}^{n+1}\right)}{\delta r_{i-1}}\right] + f\left[\frac{\rho_a}{\rho_p} k_p A_i\left(X_i^{n+1} - X_{sp}^{n+1}\right)\right] + (1-f)\left[\frac{\rho_a}{\rho_p} k_p A_i\left(X_i^{n} - X_{sp}^{n}\right)\right. \ldots\ldots\ldots \quad (71)$$

For solid Phase energy equation can be given as

$$\frac{\partial(\rho_P C_P T_P)}{\partial t} = \frac{1}{r^2}\frac{\partial}{\partial r}\left(r^2 k_{rp}\frac{\partial T_p}{\partial r}\right) \ldots\ldots\ldots\ldots\ldots\ldots\ldots\ldots\ldots\ldots \quad (72)$$

The final form of the discretization energy equation can be given as

$$\frac{[(\rho_P C_P T_P)_i^{n+1}-(\rho_P C_P T_P)_i^n]\Delta V}{4\pi\Delta t} = f\left[\frac{r^2_{i+\frac{1}{2}} k_{tp}{}_{i-\frac{1}{2}}\left(T_{p_{i+1}}^{n+1}-T_{P_i}^{n+1}\right)}{\delta r_{i+1}} - \frac{r^2_{i-\frac{1}{2}} k_{tp}{}_{i-\frac{1}{2}}\left(T_{p_i}^{n+1}-T_{P_{i-1}}^{n+1}\right)}{\delta r_{i-1}}\right]\Delta t + (1-f)\left[\frac{r^2_{i+\frac{1}{2}} k_{tp}{}_{i-\frac{1}{2}}\left(T_{p_{i+1}}^{n}-T_{P_i}^{n}\right)}{\delta r_{i+1}} - \frac{r^2_{i-\frac{1}{2}} k_{tp}{}_{i-\frac{1}{2}}\left(T_{p_i}^{n}-T_{P_{i-1}}^{n}\right)}{\delta r_{i-1}}\right]\Delta t \ldots\ldots\ldots\ldots\ldots (73)$$

To obtain the boundary condition Eq. (72) should be integrated on the surface grid of the solid considering the effect of heat transfer with interstitial gas and the wall also the latent heat due to evaporation

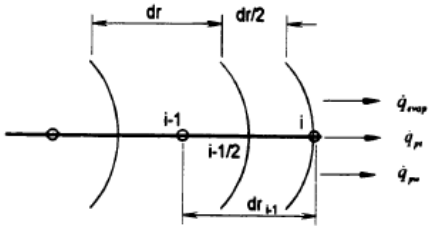

Figure 4.5 Half control Volume at boundary condition

The final form of discretization equation for boundary grid is

$$\frac{[(\rho_P C_P T_P)_i^{n+1}-(\rho_P C_P T_P)_i^n]\Delta V_i}{4\pi\Delta t} = -f\left[A_{i-\frac{1}{2}} k_{tp}{}_{i-\frac{1}{2}} \frac{\left(T_{p_i}^{n+1}-T_{P_{i-1}}^{n+1}\right)}{\delta r_i}\right] - (1-f)\left[A_{i-\frac{1}{2}} k_{tp}{}_{i-\frac{1}{2}} \frac{\left(T_{p_i}^{n}-T_{P_{i-1}}^{n}\right)}{\delta r_i}\right] + f\left[h_P A_i\left(T_i^{n+1}-T_{P_i}^{n+1}\right)\right] + (1-f)\left[h_P A_i\left(T_i^{n}-T_{P_i}^{n}\right)\right] + f\left[\rho_a k_p A_i\left(X_i^{n+1}-X_{P_i}^{n+1}\right)h_{fg}^{n+1}\right] + (1-f)\left[\rho_a k_p A_i\left(X_i^{n}-X_{P_i}^{n}\right)h_{fg}^{n}\right] + f\left[h_{pw} A_{pw}\left(T_w^{n+1}-T_{P_i}^{n+1}\right)\right] + (1-f)\left[h_{pw} A_{pw}\left(T_w^{n}-T_{P_i}^{n}\right)\right] \ldots\ldots\ldots (74)$$

5. Method of Solution

As mentioned earlier the governing partial differential equation in Fluidized bed drying are of two types generally. First-order hyperbolic partial differential equations are implemented for gas phase, and second order hyperbolic partial differential equations are used for solid phase. Since these equations show dual nature it is important to select a proper solution method. Special attention is required to converge the partial differential equation system as they are coupled and non-linear. As direct methods are non-economical they are not used for nonlinear equation. Iterative methods provide an alternative for discretized equation solution.

In order to account the axial change in the gas properties bed expansion is considered following which the gas flow rate is divided into number of control volumes. Variation inside the particles is accounted dividing the solid phase finite control volumes.

Arbitrary values for all dependent variables in the equations are assumed before starting the solution procedure. After that equation set for the first control volume of the bed is solved by employing Gauss-Seidel iterative method. The iteration continues and successive repetition of the algorithm produces a solution sufficiently close to the correct solution. After the convergence of the solution, the moisture and temperature distribution in solid as other parameters related to the gas flow inside the first control volume can be specified. The process is continued for all the control volumes.

In an aggregative fluidization state, due to bubble movement mixing of the particles in bed is continuous. An average moisture and temperature distribution of all solids in the bed is assumed as the mixing rate of particle is high whereas the time scale of mixing could be as low as gas residence time in bed. The moisture and temperature distribution of solid in each control volume may be different as the interstitial gas and bubble phase condition for each control volume is different. Average of the moisture and temperature distribution values for solid in same grid at different control volume is calculated in order to obtain an expression for the average moisture and temperature distribution in solid. So it can be said that fluidized bed was considered as a fixed bed during the numerical time step and accordingly the distribution of moisture and temperature of solids in each control volume in the bed is calculated and subsequently averaged to obtain the moisture and temperature distribution of particles at that time step.

In simulation of fixed bed drying the averaging step is not required in axial direction as the particle positions are not mixing in the bed, and their positions are fixed.

6. Under-relaxation

While solving nonlinear system of equations, the speed of the change in the dependent variable values is increased or decreased from iteration to iteration before convergence to achieve acceptable level accuracy. If the changes in the variables are accelerated the process is called over-relaxation while deceleration in the change of variable is known as under-relaxation. Over relaxation is used when the direction of the change in the solution is observed and anticipated that the same trend is valid for the following steps. It is usually suitable for numerical solution to Laplace's equation with Drichlet boundary condition. On the other hand Under-relaxation is used when the convergence at a point is taken an oscillatory pattern and tends to "overshoot" the apparent final solution. It is used for nonlinear problem to avoid divergence in the iterative solution of strongly nonlinear equation. Without under relaxation the solution may not converge to the final solution. This could be attributed to the highly nonlinear nature of the governing equation specially the sorption isotherm equation. Due to strong nonlinear behavior of the sorption isotherm equation, the solution should be able to proceed with a small change to be able to capture the nonlinear pattern of the equation. Otherwise, the solution may overshoot without convergence.

Some general guidelines for selection of best under relaxation coefficient can be given.

In the moderate temperature drying the under relaxation coefficient close to one is adequate for getting the convergence but as the temperature of drying medium rises, the under relaxation coefficient must decrease. While under relaxation helps to converge the solution it also increases the

computational time and iteration to find the required solution. Because of this it is recommended that the value of ω should be not being too small.

7. Conclusion

The mathematical model has been proposed for the fluidized bed system. Drying calculation of wheat has been done and in this work, no chemical reactions are considered in the gas phase so that there is no specific need to resolve turbulence. In mathematical modelling proposed the equations for particle phase modelling, Drying and Pyrolysis Model, Constant rate model, falling rate model. Also, Discretization of Differential Equation is given.

8. References

[1] R. Sivakumar, R. Saravanan, A. ElayaPerumal, S. Iniyan (2016) "Fluidized bed drying of some agro products – A review" Renewable and Sustainable Energy Reviews 61 (2016) 280–301

[2] S. Syahrul, I. Dincer b, F. Hamdullahpur (2002) "Thermodynamic modeling of fluidized bed drying of moist particles" International Journal of Thermal Sciences 42 (2003) 691–701

[3] WijithaSenadeera, Bhesh R. Bhandari, Gordon Young , BanduWijesinghe(2002) "Influence of shapes of selected vegetable materials on drying kinetics during fluidized bed drying" Journal of Food Engineering 58 (2003) 277–283

[4] S. Syahrul, F. Hamdullahpur, I. Dincer (2001) "Exergy analysis of fluidized bed drying of moist particles" Exergy, an International Journal 2 (2002) 87–98

[5] JanuszStanisławski (2005) Drying of Diced Carrot in a Combined Microwave–Fluidized Bed Dryer, Drying Technology: An International Journal, 23:8, 1711-1721, DOI: 10.1081/DRT-200065129

[6] Afzal, T. M., & Abe, T. (1999). Some fundamental attributes of far infrared radiation drying of potato. Drying Technology, 17(1&2), 137–155.

[7] Borgolte, G., & Simon, E. J. (1981). Fluid bed processes in the manufacture of snack products. CEB review for Chocolate, Confectionary and Bakery, 6(2), 7–8, 10.

[8] Brennan, J. G. (1994). Food dehydration: a dictionary and guide. Oxford, UK: Butterworth-Heinemann Series in Food Control.

[9] Crank, J. (1975). The mathematics of diffusion (2nd ed.). Oxford, UK: Oxford University Press.

[10] Gibert, H., Baxerres, J. L., & Kim, H. (1980). Blanching time in fluidized beds. In P. Linko, Y. Malkki, J. Olkku, & J. Larinkari (Eds.), Food process engineering 1: food processing systems (pp. 75– 85). London: Applied Science Publishers.

[11] Giner, S. A., &Calvelo, A. (1987). Modelling of wheat drying in fluidized beds. Journal of Food Science, 52(5), 1358–1363.

[12] Karthanos, V. T., Anglea, S., &Karel, M. (1993). Collapse of structure during drying of celery. Drying Technology, 11, 1005– 1023.

[13] Madamba, P. S., Driscoll, R. H., & Buckle, K. A. (1996). The thin layer drying characteristics of garlic slices. Journal of Food Engineering, 29, 75–97.

[14] Noomhorn, A., &Verma, L. R. (1986). Generalized single layer rice drying models. Transactions of the ASAE, 29(2), 587– 591.

[15] Palipane, K. B., & Driscoll, R. H. (1994). The thin layer drying characteristics of macadamia in-shell nuts and kernels. Journal of Food Engineering, 23, 129–144.

[16] Perry, R. H., Green, D. W., & Maloney, J. O. (1992). Perrys chemical engineers handbook (6th ed.). NY: McGraw-Hill.

[17] Rossello, C., Canellas, J., Simal, S., &Berna, A. (1992). Simple mathematical model to predict the drying rates of potato. Journal of Agricultural and Food Chemistry, 40(12), 2374–2378.

[18] Rossello, C., Simal, S., SanJuan, N., &Mulet, A. (1997). Nonisotropic mass transfer model for green bean drying. Journal of Agricultural and Food Chemistry, 45, 337–342.

[19] Sablani, S., Rahman, S., & Al-Habsi, N. (2000). Moisture diffusivity in foods- an overview. In A. S. Mujumdar (Ed.), Drying technology in agriculture and food sciences (pp. 35–50). Enfield, USA: Science Publishers Inc.

[20] Sawhney, R. L., Sarasavadia, P. N., Pangavhane, D. R., & Singh, S. P. (1999). Determination of drying constants and their dependence on drying air parameters for thin layer onion drying. Drying Technology, 17(1&2), 299–315.

[21] Senadeera, W., Bhandari, B., Young, G., &Wijesinghe, B. (2000). Physical properties and fluidisationbehaviour of fresh green bean particulates during fluidised bed drying. Food and Bioproducts Processing (Trans IchemE), 43–47.

[22] SAS (1985). User's Guide: Statistics, 5th ed. SAS Institute Inc., Cary, NC.